Artificial intelligence solution to accelerate the acquisition of MRI images: Impact on the therapeutic care in oncology in radiology and radiotherapy departments

Raphaëlle Karine Lemaire, Charlotte Raboutet, Thomas Leleu, Cyril Jaudet, Loise Dessoude, Fernand Missohou, Yoann Poirier, Pierre-Yves Deslandes, Alexis Lechervy, Joëlle Lacroix, et al.

Cancer/Radiothérapie xxx (xxxx) xxx–xxx

Disponible en ligne sur
ScienceDirect
www.sciencedirect.com

Elsevier Masson France
EM|consulte
www.em-consulte.com

Original article

Artificial intelligence solution to accelerate the acquisition of MRI images: Impact on the therapeutic care in oncology in radiology and radiotherapy departments

Solution d'intelligence artificielle pour accélérer l'acquisition d'images remnographiques : impact sur la prise en charge thérapeutique en oncologie dans les services de radiologie et radiothérapie

R. Lemaire[a], C. Raboutet[b], T. Leleu[c], C. Jaudet[a], L. Dessoude[c], F. Missohou[c], Y. Poirier[b], P.-Y. Deslandes[d], A. Lechervy[e], J. Lacroix[b], I. Moummad[a,f], S. Bardet[g], J. Thariat[c], D. Stefan[c], A. Corroyer-Dulmont[a,*,h]

[a] *Medical Physics Department, centre François-Baclesse, 14000 Caen, France*
[b] *Radiology Department, centre François-Baclesse, 14000 Caen, France*
[c] *Radiotherapy Department, centre François-Baclesse, 14000 Caen, France*
[d] *Informatics Department, centre François-Baclesse, 14000 Caen, France*
[e] *UMR Greyc, Normandie Université, UniCaen, EnsiCaen, CNRS, 14000 Caen, France*
[f] *IMT Atlantique, Lab-Sticc, UMR CNRS 6285, 29238 Brest, France*
[g] *Nuclear Medicine Department, centre François-Baclesse, 14000 Caen, France*
[h] *Université de Caen Normandie, CNRS, Normandie Université, ISTCT UMR6030, GIP Cyceron, 14000 Caen, France*

ARTICLE INFO

Article history:
Received 19 October 2023
Accepted 28 November 2023

Keywords:
Artificial intelligence
Radiology
Radiotherapy
Oncology

ABSTRACT

Purpose. – MRI is essential in the management of brain tumours. However, long waiting times reduce patient accessibility. Reducing acquisition time could improve access but at the cost of spatial resolution and diagnostic quality. A commercially available artificial intelligence (AI) solution, SubtleMR™, can increase the resolution of acquired images. The objective of this prospective study was to evaluate the impact of this algorithm that halves the acquisition time on the detectability of brain lesions in radiology and radiotherapy.

Material and methods. – The T1/T2 MRI of 33 patients with brain metastases or meningiomas were analysed. Images acquired quickly have a matrix divided by two which halves the acquisition time. The visual quality and lesion detectability of the AI images were evaluated by radiologists and radiation oncologist as well as pixel intensity and lesions size.

Results. – The subjective quality of the image is lower for the AI images compared to the reference images. However, the analysis of lesion detectability shows a specificity of 1 and a sensitivity of 0.92 and 0.77 for radiology and radiotherapy respectively. Undetected lesions on the IA image are lesions with a diameter less than 4 mm and statistically low average gadolinium-enhancement contrast.

Conclusion. – It is possible to reduce MRI acquisition times by half using the commercial algorithm to restore the characteristics of the image and obtain good specificity and sensitivity for lesions with a diameter greater than 4 mm.

* Corresponding author. Medical Physics Department, centre François-Baclesse, 14000 Caen, France.
E-mail address: a.corroyer-dulmont@baclesse.unicancer.fr (A. Corroyer-Dulmont).

https://doi.org/10.1016/j.canrad.2023.11.004
1278-3218/

Please cite this article as: Lemaire R, et al, Artificial intelligence solution to accelerate the acquisition of MRI images: Impact on the therapeutic care in oncology in radiology and radiotherapy departments, Cancer Radiother, https://doi.org/10.1016/j.canrad.2023.11.004

Mots clés :
Intelligence artificielle
Radiologie
Radiothérapie
Oncologie

RÉSUMÉ

Objectif de l'étude. – L'IRM est essentielle dans la prise en charge des tumeurs cérébrales. Cependant, les longs délais d'attente réduisent l'accessibilité des patients à cette modalité. La réduction du temps d'acquisition pourrait améliorer l'accès, mais au détriment de la résolution spatiale et de la qualité du diagnostic. Une solution d'intelligence artificielle disponible dans le commerce, SubtleMR™, peut augmenter la résolution des images acquises. L'objectif de cette étude prospective était d'évaluer l'impact de cet algorithme qui divise par deux le temps d'acquisition sur la détectabilité des lésions cérébrales en radiologie et radiothérapie.

Matériel et méthodes. – Les IRM pondérées en T1/T2 de 33 patients atteints de métastases cérébrales ou de méningiomes ont été analysées. Les images acquises rapidement possèdent une matrice divisée par deux qui divise par deux le temps d'acquisition. La qualité visuelle et la détectabilité des lésions des images d'intelligence artificielle ont été évaluées par des radiologues et des radiothérapeutes, ainsi que l'intensité des pixels et la taille des lésions.

Résultats. – La qualité subjective de l'image est inférieure pour les images d'intelligence artificielle par rapport aux images de référence. Cependant, l'analyse de la détectabilité des lésions montre une spécificité de 1 et une sensibilité de 0,92 et 0,77 respectivement pour la radiologie et la radiothérapie. Les lésions non détectées sur l'image d'intelligence artificielle sont des lésions d'un diamètre inférieur à 4 mm et d'un contraste de rehaussement moyen significativement plus faible après injection de gadolinium.

Conclusion. – Il est possible de diviser par deux les temps d'acquisition de l'IRM en utilisant l'algorithme commercial pour restituer les caractéristiques de l'image et obtenir une bonne spécificité et sensibilité pour les lésions de diamètre supérieur à 4 mm.

1. Introduction

Magnetic resonance imaging (MRI) is an important imaging modality tool in medicine for cancer diagnosis and treatment. Despite the presence of more than 800 MRI on French territory, the average time to obtain an appointment for this type of examination is about 32 days, higher than the waiting times desired by the 2014–2019 cancer plan of 20 days. Reducing acquisition time would increase MRI availability and reduce the time to obtain an appointment. There is therefore a real need to reduce this acquisition time to improve patient care. However, reducing acquisition time is feasible only with a reduction of the acquisition matrix or image averaging which decreases image quality [1]. Therefore, solutions to restore image quality after acquisition time reduction are needed.

Artificial intelligence (AI) and especially deep learning, a subdomain of AI, has seen an enormous advancements and application in medicine in recent years [2]. NYU Langone and Facebook AI Research collaborated on a research project called "fastMRI", which consists of open datasets and benchmarks for accelerating MRI sequence acquisition. They focused on brain and knee, and recently on prostate data [3–6]. Other applications exist for these algorithms, ranging from image denoising to improving the rendering of exam images to super-resolution [7,8]. A super-resolution algorithm has been validated by the US Food and Drug Administration for routine clinical application, SubtleMR™. This solution has reduced scan time acquisition by 40% in spinal MRI and 60% in brain MRI in multicentre and multi-MRI studies [9,10]. To the best of our knowledge, only one study assessed the application of the AI solution in assessing brain lesions, using a cohort of 25 patients, a 45% reduction in acquisition time was obtained with half of the number of phase-encode lines [11]. Despite these findings, none have addressed how the associated decrease in resolution because of the shorter acquisition time, could potentially affect tumour delineation. In addition, no information is available on the lesion size threshold for detectability when using the AI solution. As it is a resampling problem for the algorithm, the issue could be to remove or to create some lesions, especially the smaller ones. For this reason, in this prospective study, we evaluated the impact of the AI solution, which halves the acquisition time on the therapeutic management of small lesions such brain metastases.

2. Materials and methods

2.1. Patients

This prospective study was approved by the local institutional review board. Thirty-three patients presenting with brain metastases and meningioma referred to our oncological centre between August 2022 and March 2023 were included. No prior selection criterion was used; all patients referred to our centre, for diagnosis or treatment follow-up during the period, were enrolled. Post-gadolinium T1 and T2 fluid attenuated inversion recovery (FLAIR) brain imaging were performed for initial diagnosis or treatment efficacy follow-up. MR-004, a French national rule (Institut national des données de santé [INDS]) defining health research conduct guidelines was used for this study. All patients provided informed consent for the use of their data. The study population characteristics are shown in Table 1.

2.2. Magnetic resonance imaging (MRI) acquisition

MRI was performed on an Area Siemens 1.5 T magnet using a brain dedicated 16 channels coil with the patient in a supine position. Prior to the examination patients were injected with 0.2 mL/kg of Dotarem® (500 μmol/mL). After a shimming process and scout imaging scan, tumour gadolinium enhancement was detected with a post-gadolinium T1 brain sequence. T2 FLAIR sequences were also used to evaluate oedema. Each sequence was acquired in a clinical (reference, longer) and then in an accelerated way (half the time). Images obtained from the accelerated sequences were then processed with the commercial AI solution.

Table 1
Impact of an MRI artificial intelligence (AI) solution on clinical radiology and radiotherapy processes: description of the patient cohort.

Number of included patients	33
Sex	55% female
Age (years)	
Mean ± SD	66.33 ± 12.35
Range	[28–93]
Lesion origins, *n* (%)	
Brain metastases	28 (85%)
From lung cancer	12 (43%)
From breast cancer	5 (18%)
From kidney cancer	2 (7%)
From digestive cancer	1 (4%)
From melanoma	4 (14%)
From gynaecologic cancer	3 (11%)
From pancreatic cancer	1 (4%)
Meningiomas	5 (15%)
Total number of brain metastases	94
Number of brain metastases per patient	1.5 ± 0.71

SD: standard deviation.

Parameters for the clinical reference sequences and accelerated sequences are reported in Table 2.

2.3. Deep learning model

The commercially available deep learning model SubtleMR™ was used for resampling. This tool is based on a U-Net deep convolutional neural network backbone that was previously trained on a large number of paired low- and high-resolution images acquired from a variety of vendors, field strengths, and institutions. A new series with the same nominal resolution as the standard of care sequence was generated after applying the AI-enhanced algorithm. This model is used for inference, without any local fine-tuning or adaptation.

2.4. Image analysis and processing

2.4.1. Visual analysis

Reference and AI-reconstructed images were reviewed by one experienced radiologist and three experienced radiation oncologist on a Syngo.via viewing server (version VB 30A, Siemens Healthcare) and Raystation™ solution (V11.B) respectively. Readers attributed a global, whole-image quality (IQ) score to each MRI series:

- 1: poor;
- 2 or 3: moderate;
- 4: good;
- 5: very good.

2.4.2. Semi-quantitative analysis

2.4.2.1. Radiology. As part of routine image review, one radiologist evaluated the maximum length of each lesion using Syngo.via™. Comparison of this value was made between reference- and AI-reconstructed images.

2.4.2.2. Radiotherapy. Following a routine workflow in the radiotherapy department, a radiation oncologist delimited a three-dimensional volume of interest for each lesion using Raystation™ solution (V11.B). Structural similarity index measure and Jaccard index were used to compare the volume of interest delimited by the radiation oncologist on reference- and AI-reconstructed images.

2.4.2.3. Global. One dimension imaging profiles from left to right part of the brain patients were made to compare accelerated and AI reconstruction impact. First order intensity evaluation was performed using mean, standard deviation, min, max, skewness, kurtosis, signal to noise ratio and absolute contrast. Specificity and sensitivity were evaluated to control potential radiologist and radiation oncologist failure to detect lesions after AI reconstruction. Finally, to evaluate the performance of the AI solution in comparison with the twice-shorter acquired images, maps of change in pixel value between AI-reconstructed and reference images were computed with ImageJ as follows:

$$\frac{\text{abs}\left(\text{Postprocessing image} - \text{reference image}\right)}{\text{reference image}} \times 100$$

To compare difference in similarity between reference to accelerated and AI images, structural similarity index measure was used using the formula below:

$$SSIM\left(P_{\hat{Y}}, P_Y\right) = \frac{1}{N}\sum_{P_{\hat{Y}}P_Y} \frac{\left(2\mu_{P_{\hat{Y}}}\mu_{P_Y} + c_1\right)\left(2\sigma_{P_{\hat{Y}}}\sigma_{P_Y} + c_2\right)}{\left(\mu^2{}_{P_{\hat{Y}}} + \mu^2{}_{P_Y} + c_1\right)\left(\sigma^2{}_{P_{\hat{Y}}} + \sigma^2{}_{P_Y} + c_2\right)}$$

With:

- SSIM: structural similarity index measure;
- N: number of batches over which structural similarity index measure has been averaged;
- $\mu_{(P\_Y)}$ and $\mu_{(P\_\hat{Y})}$: mean of patches P_Y and $P_{\hat{Y}}$ respectively;
- $\sigma_{(P\_Y)}$ and $\sigma_{(P\_\hat{Y})}$: deviation of patches P_Y and $P_{\hat{Y}}$ respectively;
- c_1 and c_2: constants.

2.5. Statistical analyses

All data are expressed as mean ± standard deviation. Student's *t*-test was used to compare the different quantitative metrics between reference and AI-reconstructed images. All the statistical analysis were performed using python and SciPy library [12]. All python codes used in the analysis is available on https://github.com/AurelienCD/Impact-of-AI-MRI-solution-on-clinical-routine.

Table 2
Study on the impact of an MRI artificial intelligence solution on clinical radiology and radiotherapy processes: parameters of MRI acquisition sequences.

	Clinical reference sequences		Accelerated sequences	
	Post-gadolinium T1	T2 FLAIR	Post-gadolinium T1	T2 FLAIR
TR/TEeff (ms)	2070/3.15	9640/131	2070/3.15	9640/131
Angle (°)	15	150	15	150
NEX	1	1	1	1
Number of slices	208 contiguous slices	24 contiguous slices	208 contiguous slices	24 contiguous slices
Resolution (mm)	0.5 × 0.5 × 1	1.5 × 1.5 × 5	0.5 × 0.5 × 1	1.5 × 1.5 × 5
Acquisition matrix (pixels)	512 × 512	320 × 320	256 × 256	160 × 160
Acquisition time	4 min 48	2 min 21	2 min 39	1 min 24

FLAIR: fluid attenuated inversion recovery; TR: repetition time; TEeff: effective echo time; NEX: number of excitations.

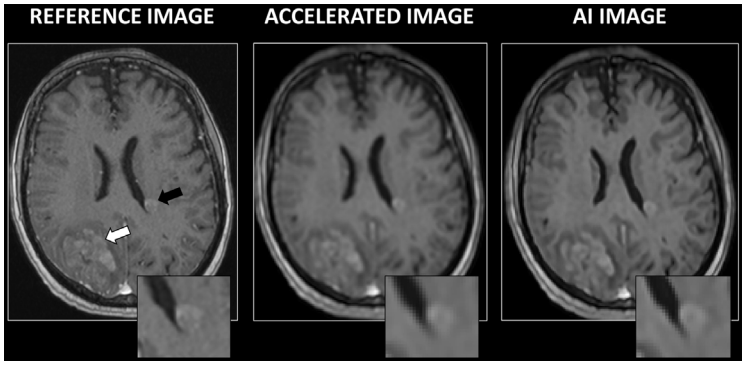

Fig. 1. Impact of an MRI artificial intelligence (AI) solution on clinical radiology and radiotherapy processes: representative images of reference, accelerated and AI-reconstructed MRI of a brain with metastases. Large (white arrow) and small (black arrow) lesions were distinguishable after the AI reconstruction process.

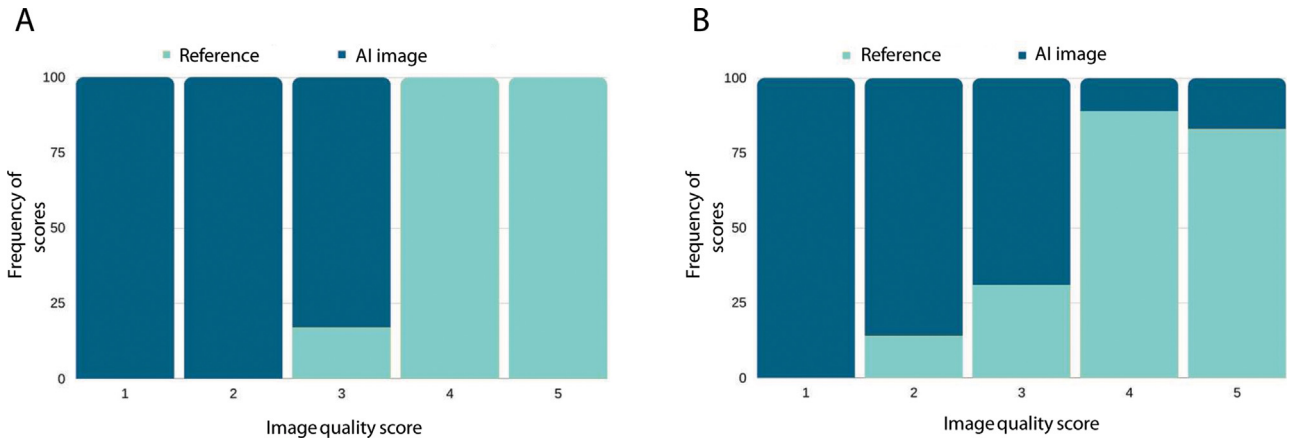

Fig. 2. Impact of artificial intelligence (AI) reconstruction on visual MRI image quality. A, B: image quality score frequencies for reference- and AI-reconstructed MRI based on radiologist (A) and radiation therapist (B) notations. 1: poor; 2, 3: moderate; 4: good; 5: very good.

3. Results

3.1. Visual analysis

The accelerated image with an acquisition matrix divided by two, presents with low resolution as illustrated in Fig. 1. AI reconstruction improves some details in the image with large lesion (white arrow) easily distinguishable but smaller lesion (black arrow) suffering from loss of detail.

Radiologist image quality scores are presented in Fig. 2A. Due to the loss of detail during the fast acquisition process not fully recovered by the AI solution, radiologist image quality scores are lower for AI images compared to reference images (mean score 4.79 ± 0.43 versus 1.86 ± 0.77, $P < 0.001$ for reference and AI images, respectively). As presented in Fig. 2B, radiation oncologist also evaluated the image quality of the reference and AI images. Results are similar but some AI image had the higher image quality score (mean score 3.94 ± 0.87 versus 2.72 ± 0.89, $P < 0.001$ for reference and AI images, respectively).

Further analysis of the differences between the three image groups showed that right to left axial profile showed a better the ability of the AI solution to recover spatial variation initially lost by the accelerated acquisition (Fig. 3A). As presented in Fig. 3B, images obtained with accelerated acquisition resulted in few variations of signal intensity throughout the axial profile. Differences were observed between the signal differences in the centre region corresponding to the cerebral ventricles for the reference image and the accelerated image (light blue line versus dark blue line in Fig. 3B). More interestingly, AI images reconstructed from the accelerated image acquisition was comparable to the reference image with similar amplitude variation, showing the ability of the AI solution to restore lost information (blue line versus light blue line in Fig. 3B).

3.2. Semi-quantitative analysis

First order signal intensity analysis of the whole image was firstly performed and revealed a decrease in mean pixel value in accelerated and AI-reconstructed images in comparison to reference images ($P < 0.001$, Table 3). No difference was found for minimal, maximal and skewness values whereas kurtosis decrease significantly ($P < 0.001$). Interestingly, signal to noise ratio increased significantly in the AI image in comparison to reference image ($P < 0.05$).

To evaluate the ability of the AI solution to restore details lost by the accelerated images, difference maps between accelerated and reference and AI and reference were computed. Fig. 4 illustrates the pixel value difference between the reference, accelerated and AI images. The reference and accelerated image subtraction map notes a 60% difference in pixel values in the contrast enhanced area. Interestingly, the AI solution was able to restore the shape of the lesion with pixel value differences lower than 30%. Structural similarity index measure was then evaluated to compare the similarity of accelerated and AI images to the reference. As shown by Fig. 4, structural similarity index measure was significantly higher in AI images in comparison to accelerated images (SSIM: 0.5921 ± 0.0577 versus 0.5878 ± 0.0588, $P < 0.01$ for AI and accelerated images, respectively).

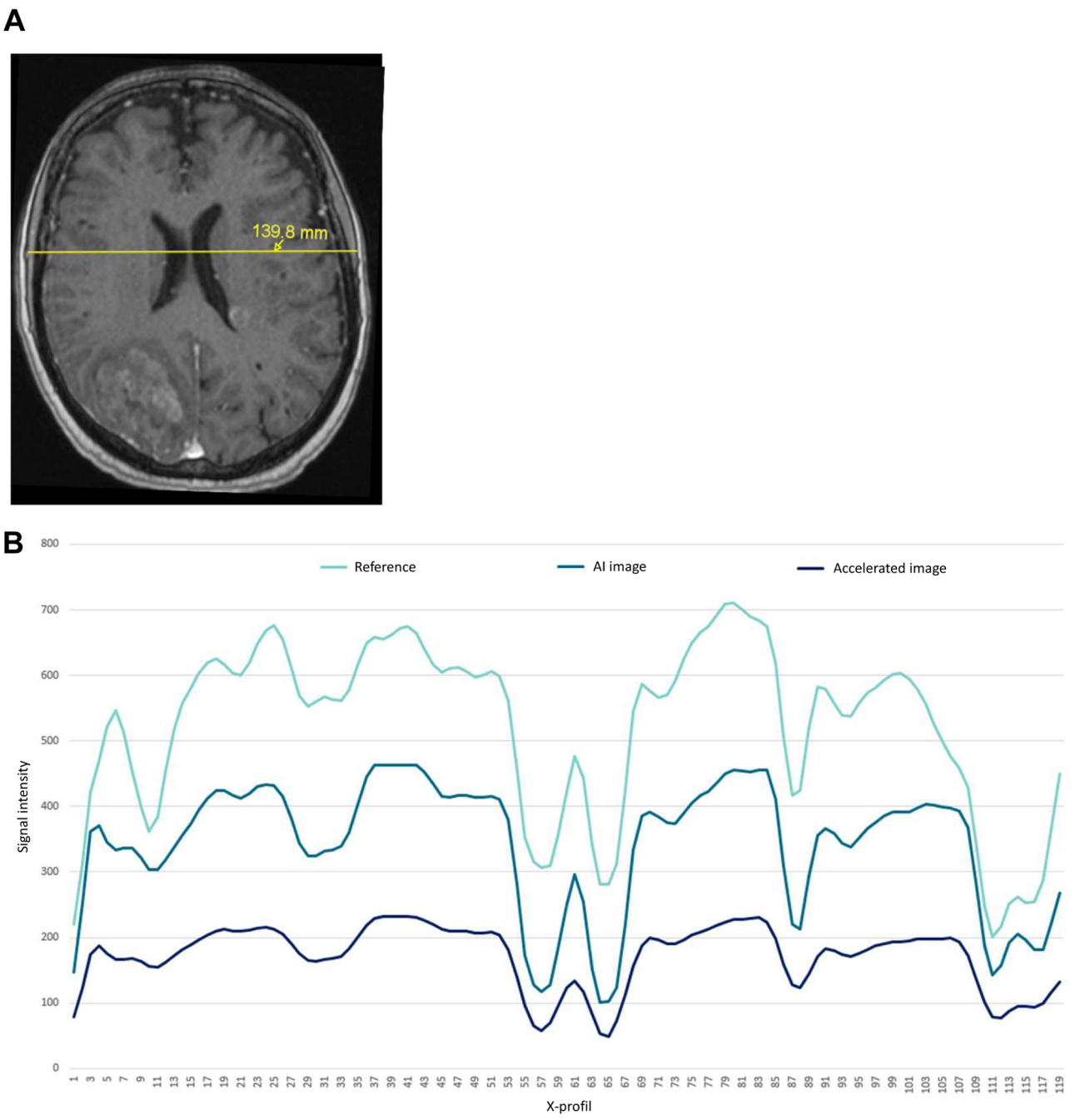

Fig. 3. Impact of an MRI artificial intelligence (AI) solution on clinical radiology and radiotherapy processes. A. Brain MRI, accelerated acquisition. B. Axial profile signal intensity for representative reference, accelerated and AI-reconstructed images.

Table 3
Impact of an MRI artificial intelligence (AI) solution on clinical radiology and radiotherapy processes: semi-quantitative analysis of the signal intensity in the global image.

	Mean (SD)	Minimum	Maximum	Skewness	Kurtosis	Signal to noise ratio
Reference image	189 (61.40)	203.6	626.5	−0.45	2.27	0.46
Accelerated image	165.73 (58.75)***	178.5	514.7	−0.46	0.29***	0.71*
AI image	166.91 (56.15)***	179.2	506.6	−0.49	0.29***	0.70*

SD: standard deviation.*$p < 0.05$; **$p < 0.01$; ***$p < 0.001$.

3.3. Impact of the AI solution on the detectability of the lesions

In this section, we evaluated lesion detectability as part of the routine clinical assessment by radiologists and radiation oncologists. Radiologists evaluate the lesion max diameter while radiation oncologists volumetrically outline three-dimensional lesions for radiotherapy planning purposes.

3.3.1. Impact of AI solution on radiology department

As presented in Fig. 5, lesion maximal diameters are similarly drawn by the radiologist in reference and in AI images. No statistical difference was observed in maximal lesion diameter (mean lesion maximal diameter: 15.35 ± 16.60 mm versus 14.38 ± 14.62 mm). However, two lesions were not detected by the radiologist in the AI images in comparison to the lesions detected using the reference

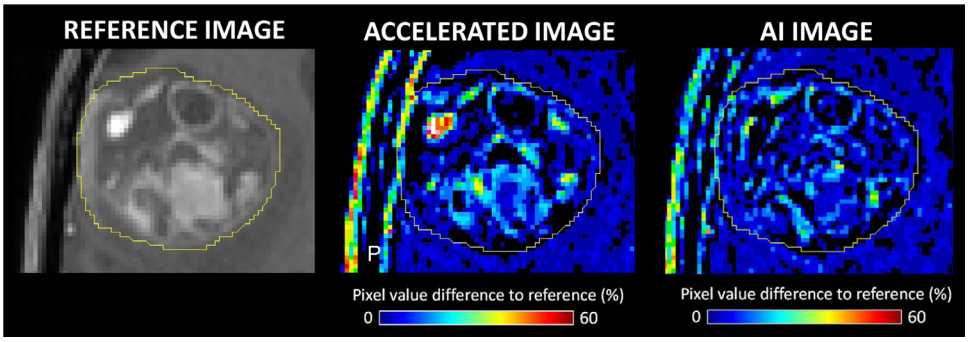

Fig. 4. Impact of an MRI artificial intelligence (AI) solution on clinical radiology and radiotherapy processes: effect of accelerated acquisition and AI solution on brain metastases signal intensity. Representative images of reference (left), difference map with accelerated acquisition (middle) and AI reconstruction MRI (right).

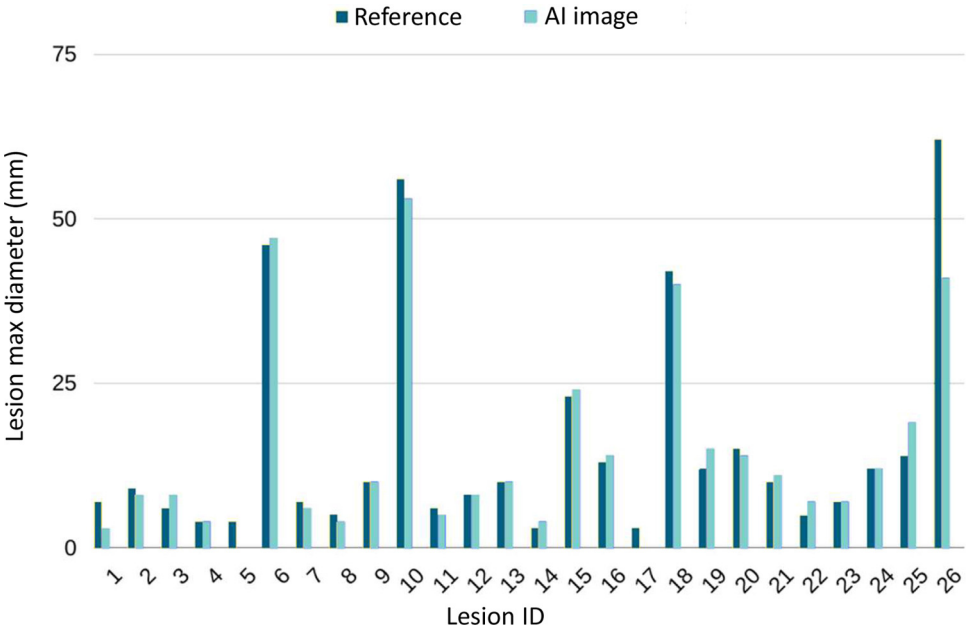

Fig. 5. Use of MRI artificial intelligence (AI) solution in clinical radiology and radiotherapy processes: impact of AI solution on maximal lesion diameters delimitation by radiologists.

lesion. This result leads to a specificity of 1 and a sensitivity of 0.92 in comparison to reference images. However, if we analyse the lesions missed by the radiologist in the AI images, it appeared that these lesions are the smaller in dimension with maximal lengths of 3 and 4 mm respectively. These results highlight the presence of a threshold for minimum lesions size to be detected of 4 mm.

3.3.2. Impact of AI solution on radiotherapy department

No significant differences were observed between volumes of interest drawn by the radiation oncologist on reference and AI images. However, five lesions were missed by the radiation oncologist in AI images in comparison to the reference images. Specificity and sensitivity were respectively 1 and 0.77. As for the radiology part, lesions missed were smaller in dimension, with volumes below 0.12 cm^3. It can also be noted that these lesions have a significant lower contrast enhancement in comparison to the other lesions (absolute contrast 0.007 ± 0.0028 versus 0.0154 ± 0.0074 for AI and reference images respectively, $P < 0.05$).

4. Discussion

MRI acquisition times that are too long lead to a long waiting time for patients in urgent need of medical interventions. Many research groups, MRI manufacturers or even start-up companies are developing solutions to enable faster acquisition without losing the diagnostic quality of the images. In our study, we analysed one of these solutions, SubtleMR™. We specifically evaluated whether this solution is able to reconstruct an image acquired two times faster than the acquisition time in clinical routine without appreciable loss in image quality as required for the routine clinical management of these patients.

Image reconstruction time using SubtleMR™ was about 1 min 30 s, which is 30 s longer than previously reported in literature [9]. This difference could be explained by the fact that the AI solution was performed on a remote computer, not directly on a graphics processing unit connected to the MRI. However, images transfer and processing did not require human intervention and therefore fits into a clinical workflow.

Regarding the visual analysis, Bash et al. have shown similar image quality for reference and AI-reconstructed images [9]. In our study, radiologists and radiation oncologists found lower image quality for AI images. This difference with the literature may be due to the fact that the matrix is only divided by two on the phase encoding axis where we have chosen to divide it on the *x* and the *y*-axes to give a significant time acquisition reduction. However, as for the cited study, we show that the AI solution is able to restore image details, which were lost during the accelerated acquisition process.

Since the images used for testing in this study were acquired on a different MRI than that used to train SubtleMR™, an adaptation of the learned features to capture the characteristics of the different MRI could potentially improve results. The participants of the fastMRI 2020 challenge pointed out that fine-tuning is required before application to clinical data [5]. Sarasaen et al. have shown that when transferring a model trained on a benchmark dataset, fine-tuning on a new MRI with one subject-specific prior planning scan improves the reconstruction quality [13]. Hu et al. showed that fine-tuning reduces aliasing artefacts while also increasing peak signal to noise ratio, structural similarity index measure and decreasing normalized root mean squared error [14].

Concerning the semi-quantitative analysis, in literature studies the values of signal intensity collected on the AI image are generally closer to the values in the reference image, than to that of the accelerated image [7,15]. In our study, the phenomenon is also present. This observation was also valid for standard deviation, kurtosis and signal to noise ratio. Signal to noise ratio increases because of a decrease in the noise in the AI-reconstructed images as shown by other studies [16]. In comparison to the study by Jin et al., our results showed structural similarity index measure with reference images higher in AI images in comparison to accelerated images [8].

Concerning the impact of the AI solution on lesion detectability and delineation, maximal diameters and three-dimension delimitations by radiologist and radiation oncologist respectively were not significantly different using reference or AI images. This conclusion is in line with the literature showing that AI solutions need to be improved but are sufficient to safely use in clinical routine [2]. As we have shown in a previous study using an AI solution with positron-emission tomography imaging, missed lesions correspond only to small lesions with low radiotracer uptake that will have limited impact on the clinical therapeutic care and patient outcome [17].

Finally, it is important to balance the performance of an AI solution applied on final MRI images in comparison to an AI algorithm developed using a raw MRI signal as K-space. In the literature, several articles use K-space images as input with better results, because more information can be found in that image rather than final MRI image [18–20]. However, in a clinical situation it is often not possible to have routine access to the k-space except for directly embedded AI solutions from the manufacturer.

5. Conclusion

In a busy MRI clinical department, the AI solution could be used to great effect to increase patient throughput without an appreciable decrease in resolution. This was demonstrated in the comparable assessment of brain lesions with diameters greater than 4 mm by oncologists and radiologists alike. Future multicentric studies, including other MRI sequences and tumour sites, are warranted.

Disclosure of interests

The authors did not disclose their relationships/activities/interests.

Funding

This study was funded by Région Normandie (France), with Booster IA grant.

Acknowledgements

The authors thank Dr Nadia Falzone for her useful comments and technical advice on the manuscript.

References

[1] Obuchowicz R, Piórkowski A, Urbanik A, Strzelecki M. Influence of acquisition time on MR image quality estimated with nonparametric measures based on texture features. Biomed Res Int 2019;2019:3706581, http://dx.doi.org/10.1155/2019/3706581.
[2] Johnson PM, Recht MP, Knoll F. Improving the speed of MRI with artificial intelligence. Semin Musculoskelet Radiol 2020;24:12–20, http://dx.doi.org/10.1055/s-0039-3400265.
[3] Zbontar J, Knoll F, Sriram A, Murrell T, Huang Z, Muckley MJ, et al. fastMRI: an open dataset and benchmarks for accelerated MRI. ArXiv [Preprint] 2018:1–35 http://arxiv.org/abs/1811.08839.
[4] Knoll F, Zbontar J, Sriram A, Muckley MJ, Bruno M, Defazio A, et al. fastMRI: A publicly available raw k-space and DICOM dataset of knee images for accelerated MR image reconstruction using machine learning. Radiol Artif Intell 2020;2:e190007, http://dx.doi.org/10.1148/ryai.2020190007.
[5] Muckley MJ, Riemenschneider B, Radmanesh A, Kim S, Jeong G, Ko J, et al. Results of the 2020 fastMRI challenge for machine learning MR image reconstruction. IEEE Trans Med Imaging 2021;40:2306–17, http://dx.doi.org/10.1109/TMI.2021.3075856.
[6] Tibrewala R, Dutt T, Tong A, Ginocchio L, Keerthivasan MB, Baete SH, et al. FastMRI prostate: a publicly available, biparametric MRI dataset to advance machine learning for prostate cancer imaging. ArXiv [Preprint] 2023 [Update in: Sci Data 2024;11:404] https://arxiv.org/abs/2304.09254.
[7] Moummad I, Jaudet C, Lechervy A, Valable S, Raboutet C, Soilihi Z, et al. The impact of resampling and denoising deep learning algorithms on radiomics in brain metastases MRI. Cancers (Basel) 2021;14:36, http://dx.doi.org/10.3390/cancers14010036.
[8] Jin Z, Xiang QS. Improving accelerated MRI by deep learning with sparsified complex data. Magn Reson Med 2023;89:1825–38, http://dx.doi.org/10.1002/mrm.29556.
[9] Bash S, Johnson B, Gibbs W, Zhang T, Shankaranarayanan A, Tanenbaum LN. Deep learning image processing enables 40% faster spinal MR scans which match or exceed quality of standard of care: a prospective multicenter multireader study. Clin Neuroradiol 2022;32:197–203, http://dx.doi.org/10.1007/s00062-021-01121-2.
[10] Bash S, Wang L, Airriess C, Zaharchuk G, Gong E, Shankaranarayanan A, et al. Deep learning enables 60% accelerated volumetric brain MRI while preserving quantitative performance: a prospective, multicenter, multireader trial. AJNR Am J Neuroradiol 2021;42:2130–7, http://dx.doi.org/10.3174/ajnr.A7358.
[11] Rudie JD, Gleason T, Barkovich MJ, Wilson DM, Shankaranarayanan A, Zhang T, et al. Clinical assessment of deep learning-based super-resolution for 3D volumetric brain MRI. Radiol Artif Intell 2022;4:e210059, http://dx.doi.org/10.1148/ryai.210059.
[12] Anon. Anaconda Software Distribution; 2020. https://docs.anaconda.com.
[13] Sarasaen C, Chatterjee S, Breitkopf M, Rose G, Nürnberger A, Speck O. Fine-tuning deep learning model parameters for improved super-resolution of dynamic MRI with prior-knowledge. Artif Intell Med 2021;121:102196, http://dx.doi.org/10.1016/j.artmed.2021.102196.
[14] Hu Y, Xu Y, Tian Q, Chen F, Shi X, Moran CJ, et al. RUN-UP: Accelerated multishot diffusion-weighted MRI reconstruction using an unrolled network with U-Net as priors. Magn Reson Med 2021;85:709–20, http://dx.doi.org/10.1002/mrm.28446.
[15] Zhao C, Shao M, Carass A, Li H, Dewey BE, Ellingsen LM, et al. Applications of a deep learning method for anti-aliasing and super-resolution in MRI. Magn Reson Imaging 2019;64:132–41, http://dx.doi.org/10.1016/j.mri.2019.05.038.
[16] Kashiwagi N, Tanaka H, Yamashita Y, Takahashi H, Kassai Y, Fujiwara M, et al. Applicability of deep learning-based reconstruction trained by brain and knee 3T MRI to lumbar 1.5T MRI. Acta Radiol Open 2021;10, http://dx.doi.org/10.1177/20584601211023939.
[17] Weyts K, Lasnon C, Ciappuccini R, Lequesne J, Corroyer-Dulmont A, Quak E, et al. Artificial intelligence-based PET denoising could allow a two-fold reduction in (18F)-FDG PET acquisition time in digital PET/CT. Eur J Nucl Med Mol Imaging 2022;49:3750–60, http://dx.doi.org/10.1007/s00259-022-05800-1.
[18] Lin DJ, Johnson PM, Knoll F, Lui YW. Artificial intelligence for MR image reconstruction: an overview for clinicians. J Magn Reson Imaging 2021;53:1015–28, http://dx.doi.org/10.1002/jmri.27078.
[19] Recht MP, Zbontar J, Sodickson DK, Knoll F, Yakubova N, Sriram A, et al. Using deep learning to accelerate knee MRI at 3 T: results of an interchangeability study. AJR Am J Roentgenol 2020;215:1421–9, http://dx.doi.org/10.2214/AJR.20.23313.
[20] Clifford B, Conklin J, Huang SY, Feiweier T, Hosseini Z, Goncalves Filho ALM, et al. An artificial intelligence-accelerated 2-minute multishot echo planar imaging protocol for comprehensive high-quality clinical brain imaging. Magn Reson Med 2022;87:2453–63, http://dx.doi.org/10.1002/mrm.29117.